

This is a repository copy of *Absorptive scattering model for rough laminar surfaces*.

White Rose Research Online URL for this paper:

<https://eprints.whiterose.ac.uk/115958/>

Version: Accepted Version

Proceedings Paper:

Dahlan, H. A. and Hancock, E. R. orcid.org/0000-0003-4496-2028 (2016) Absorptive scattering model for rough laminar surfaces. In: Davis, L., Bimbo, A. Del and Lovell, B., (eds.) 2016 23rd International Conference on Pattern Recognition (ICPR). IEEE Computer Society , Los Alamitos, CA, USA , pp. 1905-1910.

<https://doi.org/10.1109/ICPR.2016.7899915>

Reuse

Items deposited in White Rose Research Online are protected by copyright, with all rights reserved unless indicated otherwise. They may be downloaded and/or printed for private study, or other acts as permitted by national copyright laws. The publisher or other rights holders may allow further reproduction and re-use of the full text version. This is indicated by the licence information on the White Rose Research Online record for the item.

Takedown

If you consider content in White Rose Research Online to be in breach of UK law, please notify us by emailing eprints@whiterose.ac.uk including the URL of the record and the reason for the withdrawal request.

Absorptive Scattering Model for Rough Laminar Surfaces

Hadi A. Dahlan and Edwin R. Hancock

Department of Computer Science, University of York,
Deramore Lane, York, YO10 5GH

Abstract—This paper introduces a new light scattering model for surfaces with rough boundaries and absorption. This is an extension to Ragheb-Hancock model. The new model adds an absorption term proportional of the squared cosine of the light incidence angle, and satisfies conservation of energy. To test the accuracy of the model, we have used the CURET database. The model was compared with alternatives such as the Jensen model, the Oren-Nayar model, and the original Ragheb-Hancock model. The results show that the new model produces the best fits to the data. Interestingly the model is capable of predicting absorption in dominant colored samples, a feature not possible with the original models studied. The absorption parameter of the new model provides is also informative of surface structure and composition, especially for layered dielectric materials.

I. INTRODUCTION

Light scattering models are of strong current interest in surface analysis for computer vision and graphics. The difficulty in predicting how light scatters from surfaces has stimulated the investigation of different modelling approaches for specific types of surface. For light scattering from rough surfaces, there are multiple parameters that contribute to the scattering behavior, and which must be considered. An effective model must consider all the relevant physical surface parameters. Unfortunately some of these can prove difficult to control or impractical to measure. These parameters are often ignored in surface modelling, and this, in turn, limits the effectiveness of the underlying model

Light absorption measurements are especially useful for modeling and analyzing the chromatic properties of materials. They also have significant application in the biomedical imaging domain. In this paper we therefore aim to improve on existing light scattering models, and develop a modified version of the Ragheb-Hancock light scattering model for layered rough surface [1], by adding a wavelength dependant absorption term.

II. OVERVIEW

A. Prior Work

The Bidirectional Reflectance Distribution Function (BRDF) [2] [3] is a general tool for characterizing light reflectance distributions from different surfaces. The function describes the angular distribution of reflected radiance in terms of the corresponding distribution of incident radiance. Most existing models are developments or refinements of the classical Phong model, Torrance-Sparrow model, or the

Oren-Nayar model, including terms for specular and diffuse reflectance [3].

Torrance and Sparrow first introduced a model for specular reflection from rough surfaces [4] [3]. Here roughness is modelled using microscopic concavities which have a V-form and are of equal length, referred to as microfacets. The microfacets have random orientations whose distribution is controlled by a number of model parameters. The model allows surfaces of varying degrees of roughness to be simulated. The Torrance-Sparrow model is considered as precursor to more recent scattering models. For instance, Oren and Nayar [5] developed a diffuse reflectance model, based on [4]. It is an improved version of the classic Lambertian interpretation of light scattering from diffuse materials, where each microfacet follow Lambert's law and which can be derived using geometrical optics.

In nature, many dielectric surfaces have a lamellar structure, and are composed of translucent and opaque layers, each exhibiting their own roughness. Other models that aim to account for the scattering effects in layered surfaces are: a) the Stam model [6] which critically analyzes the problem of scattering in rough layered surfaces; b) the Matusik et al [7] model which makes empirical BRDF estimates for both metals and dielectrics; and c) the Ragheb and Hancock [1] model which details light scattering for layered rough dielectric surfaces. However, none of these models have taken light absorption into account.

The parameter of the absorption model is important for accurately reproducing the chromatic properties of materials and also for analyzing material absorption characteristics. It is also important for modelling and analyzing biological materials such as human skin, which not only improves the synthesis of realistic surface appearance but can also be used for the analysis of such surfaces [8]. Donner et al [9] introduce a layered, heterogeneous spectral reflectance model for human skin which accounts for absorption by introducing infinitesimally thin absorbing layers between the scattering layers. Jensen et al. [10] use the absorption coefficient in their subsurface scattering synthesis model. Both of these models use an absorption term that is designed according to the domain specific aims of the study in hand. However, the chosen parameters can be intractable to measure directly or to estimate. Based on this observation in this paper we propose a new unit-less absorption model whose parameters are more

easily estimated and which is hence to easier to control.

B. Contribution

The new model presented in this paper is a modification of the Ragheb and Hancock light scattering model for layered dielectrics with rough surface boundaries [1]. Using the wave scattering theory, the model assumes that the diffuse radiance is scattered from bi-layered rough surfaces, consisting of an opaque sub-surface layer below a transparent one. The model is detailed and produces remarkably good agreement with the experimental data studied. However, unlike our improved model, their model does not account for absorption. Hence, the new model introduced here is an extension or the Ragheb and Hancock model with the inclusion of an absorption term which is derived using the conservation energy for light transmission, reflectance, and absorption. This simplifies the analysis of reflectance without overcomplicating the model. Moreover, the absorption parameter is unit-less, and provides an alternative representation of light absorption in a dielectric.

III. METHODOLOGY

A. Ragheb and Hancock's Light Scattering Model for Rough Layered Dielectric

The surface scattering geometry of the Ragheb's model [1] was based on Kirchoff theory, as shown in Fig. 1 (a). The vector S points in the direction of the light source, which means that incident light with radiance L_i propagates in the $-S$ direction. The scattered radiance L_o is in the direction V , which is the position of the viewer. The light beam is incident on the surface with zenith angle θ_i and azimuth angle ϕ_i . Additionally, Beckmann's geometry applies so $\phi_i = \pi$ [1]. The light beam is then scattered at zenith angle θ_s and azimuth angle ϕ_s .

In the layered surface geometry under study, in Fig. 1 (b) i) light first enters the surface at angle θ_i , ii) is then refracted to angle θ'_i , iii) then undergoes single scattering on the lower surface layer (lower boundary), at angle θ'_s , and iv) finally exits the surface layer (upper boundary) with zenith and azimuth angles θ_s and ϕ_s . Both of the outgoing radiance components (surface and subsurface) are identical. The total outgoing radiance is the linear combination of both components with β as its relative balance control. The notation used is summarized in Table I.

In [1], two different surface roughness model variants are studied, referred to as i) the Gaussian and ii) the Exponential, which refer to the nature of the correlation function for the surface and subsurface roughness. The scattered surface radiance $L_o^{sf}(\theta_i, \theta_s, \phi_s, \sigma/T)$ (which we refer to as L_o^{sf}) when the surface correlation function is Gaussian and is given by:

$$L_G^{sf} = K_G \left[\frac{\cos(\theta_i)}{v_z^2(\theta_i, \theta_s)} \right] \times \exp \left[\frac{-T^2 v_{xy}^2(\theta_i, \theta_s, \phi_s)}{4\sigma^2 v_z^2(\theta_i, \theta_s)} \right] \quad (1)$$

and when surface correlation function is Exponential:

$$L_E^{sf} = K_E \left[\frac{\cos(\theta_i)}{v_z^2(\theta_i, \theta_s)} \right] \times \left(1 + \left[\frac{T^2 v_{xy}^2(\theta_i, \theta_s, \phi_s)}{\sigma^2 v_z^2(\theta_i, \theta_s)} \right] \right)^{-\frac{3}{2}} \quad (2)$$

where $v_{xy}^2(\theta_i, \theta_s, \phi_s) = [k(\sin(\theta_i) - \sin(\theta_s) \cos(\phi_s))]^2 + [-k(\sin(\theta_s) \sin(\phi_s))]^2$; $v_z(\theta_i, \theta_s) = -k(\cos(\theta_i) - \cos(\theta_s))$; and $k = 2\pi/\lambda$. The coefficients K_G and K_E are both proportional to $(\sigma/T)^2$ and can be normalized.

Meanwhile, the subsurface scattered radiance $L_o^{sb}(\theta_i, \theta_s, \phi_s, \sigma'/T', n)$ (which we refer to as L_o^{sb}) when the correlation function is Gaussian is given by:

$$L_G^{sb} = L_G^{sf}(\theta'_i, \theta'_s, \phi_s, \sigma'/T') \times [1 - f(\theta_i, n)][1 - f(\theta'_s, 1/n)] d\omega' \quad (3)$$

and when the subsurface correlation function is Exponential:

$$L_E^{sb} = L_E^{sf}(\theta'_i, \theta'_s, \phi_s, \sigma'/T') \times [1 - f(\theta_i, n)][1 - f(\theta'_s, 1/n)] d\omega' \quad (4)$$

where, the solid angle is:

$$d\omega' = \frac{\cos(\theta_i)}{n^2 \cos(\theta'_i)} d\omega \quad (5)$$

where the Fresnel coefficient, which models the refraction effects of the layers is given

$$f(\alpha_i, r) = \left[\frac{\sin^2(\alpha_i - \alpha_t)}{2 \sin^2(\alpha_i + \alpha_t)} \right] \times \left[1 + \frac{\cos^2(\alpha_i + \alpha_t)}{\cos^2(\alpha_i - \alpha_t)} \right] \quad (6)$$

$$r = \frac{\sin(\alpha_i)}{\sin(\alpha_t)} \quad \text{and} \quad \alpha_t = \sin^{-1} \left[\frac{\sin(\alpha_i)}{r} \right] \quad (7)$$

In equation (7), where light is transmitted from air to dielectric, then $r = n$ and $\alpha_i = \theta_i$. If, on the other hand, light is transmitted from dielectric to air, then $r = 1/n$ and $\alpha_i = \sin^{-1}[\sin(\theta_s)/n]$. The overall outgoing scattered radiance L_o is then given by:

$$L_o = \beta L_o^{sb} + (1 - \beta) L_o^{sf} \quad (8)$$

B. Absorption In the Subsurface Layer

To convey the degree of light absorption in a material, different measurements can be used. One example is the complex refractive index, which was used in Mie Theory to describe the absorption of electromagnetic radiation by spherical particles [11]. However, deriving a light scattering or reflectance model using the parameter can be difficult, resulting from problems either in measuring its value or solving for its imaginary component.

Instead of using a predefined function as the absorption term (e.g. complex refractive index), our new model derives the absorption term from first principles using the principle of conservation of energy during light transfer. In Ragheb and Hancock's model, the reflectance is governed by the Fresnel co-efficient and the conservation energy was assumed to be

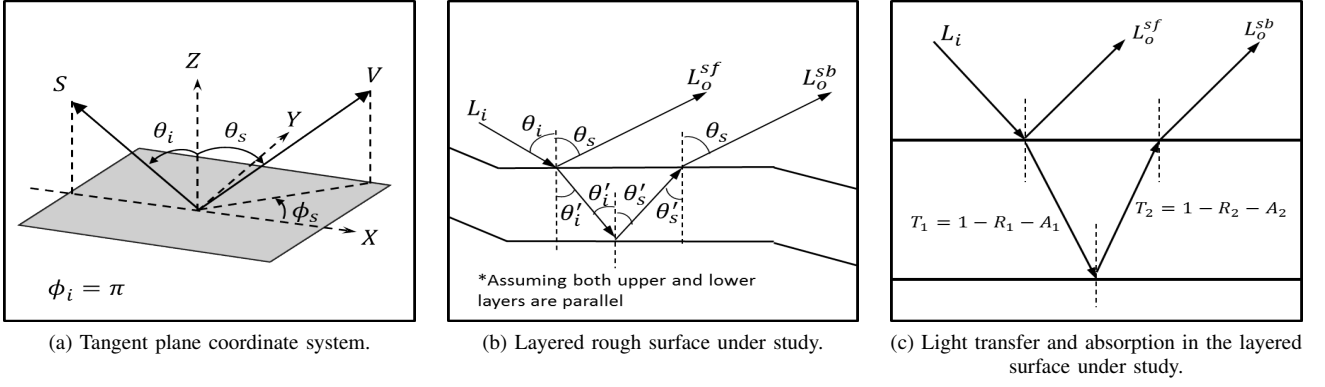


Fig. 1. The scattering geometry.

 TABLE I
 FORMULA NOTATION.

Notation	Description
L_i	Incident radiance
L_o	Total scattered radiance
L_G^{sf}	Surface scattered radiance with Gaussian correlation function
L_G^{sb}	Subsurface scattered radiance with Gaussian correlation function
L_E^{sf}	Surface scatter radiance with Exponential correlation function
L_E^{sb}	Subsurface scattered radiance with Exponential correlation function
θ_i	Surface incident zenith angle
θ_s	Surface scattering zenith angle
θ'_i	Subsurface incident zenith angle
θ'_s	Subsurface scattering zenith angle
ϕ_s	Scattered azimuth angle
σ/T	Surface RMS slope
σ'/T'	Subsurface RMS slope
K_G or K_E	Coefficients for the surface equations of Gaussian and Exponential respectively
$d\omega'$	Solid angle under mean surface level
n	Standard refractive index
β	Balance parameter

satisfied provided the normalisation $1 = R + T$ held. However, for the new model, the conservation energy is expressed via the different normalisation:

$$1 = R + T + A \quad (9)$$

In this equation, the amount of absorbed light A is assumed to be proportional to the cosine squared of the incident angle θ_i . As a result, the absorption is greatest (100%) when the incident light is normal to the surface and smallest (0%) when the incident light is perpendicular to the surface normal. The absorption term is defined as:

$$A_1 = A(a, \theta_i) = a(\cos^2(\theta_i))[1 - f(\theta_i, n)] \quad (10)$$

$$A_2 = A(a, \theta_{s2}) = a(\cos^2(\theta_{s2}))[1 - f(\theta'_s, 1/n)] \quad (11)$$

where a is the fractional absorption parameter, used to control how strongly light is absorbed. Equation 10 is used when

incident light is transmitted from air to the material. On the other hand, Equation 11 is used when the incident light is transmitted from the material to air. Substituting (10) and (11) into (3) and (4), the subsurface scattering component now becomes:

$$L_G^{sb}(\theta_i, \theta_s, \phi_s, \sigma'/T', n) = L_G^{sf}(\theta'_i, \theta'_s, \phi_s, \sigma'/T') \times [1 - f(\theta_i, n) - A(a, \theta_i)][1 - f(\theta'_s, 1/n) - A(a, \theta_{s2})]d\omega' \quad (12)$$

$$L_E^{sb}(\theta_i, \theta_s, \phi_s, \sigma'/T', n) = L_E^{sf}(\theta'_i, \theta'_s, \phi_s, \sigma'/T') \times [1 - f(\theta_i, n) - A(a, \theta_i)][1 - f(\theta'_s, 1/n) - A(a, \theta_{s2})]d\omega' \quad (13)$$

where

$$\theta_{s2} = \sin^{-1} \left[\frac{\sin(\theta'_s)}{1/n} \right] \quad (14)$$

By conservation of energy, a change in the absorption will cause a change in the transmission. Fig. 2 shows how the different values of a affect the behavior of both the transmission and the absorption as the incident angle varies (for a medium with $n = 1.7$).

IV. EXPERIMENTAL SETUP AND RESULTS

To test our model, we use the CURET database [12]. Here we excluded the BRDF measurements that occur in the specular direction, and which total 198 non-specular measurements. In total 13 different material samples were selected for the experiment. The test was performed on the colour channels of the different samples (RGB), giving a total of 39 sample BRDF's. Before the fitting, the tabulated BRDF data $v(\theta_i, \phi_i, \theta_s, \phi_s)$ were converted into normalized outgoing radiance $L_o(\theta_i, \phi_i, \theta_s, \phi_s)$ using $L_o(\theta_i, \phi_i, \theta_s, \phi_s) = v(\theta_i, \phi_i, \theta_s, \phi_s)L_i \cos(\theta_i)d\omega$. We experimented with fitting four different models to the the CURET data, namely a) the proposed model with an Exponential correlation function, b) the proposed model with Gaussian correlation function, c) the Jensen model and d) the Oren-Nayar model. The different models are used to explore how the absorption parameter affects the overall quality of fit.

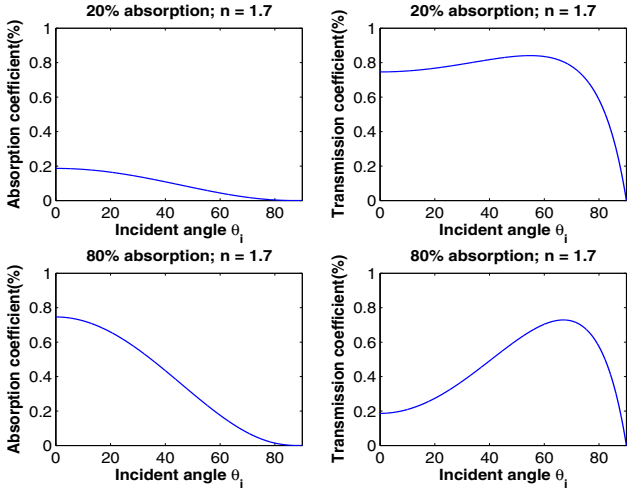


Fig. 2. The Absorption and Transmission curve behavior.

A. Model Fitting

The normalized predicted radiance of the models is fitted to the normalized measured radiance data from the CUREt database. This is done by varying the model parameters to find their smallest value of the root-mean-square error Δ_{RMS} . The RMS fitting error is given by:

$$\Delta_{RMS} = 100 \times \frac{1}{K} \left\{ \sum_{k=1}^K \left[L_O^D(\theta_i^k, \phi_i^k, \theta_s^k, \phi_s^k) - L_O^P\left(\theta_i^k, \phi_i^k, \theta_s^k, \phi_s^k, \frac{\sigma}{T}, \frac{\sigma'}{T'}, n, \beta\right) \right]^2 \right\}^{\frac{1}{2}} \quad (15)$$

where L_O^D is the normalized BRDF from the CUREt database, L_O^P is the normalized radiance from the model prediction and k runs over the index number of the BRDF measurements used (K).

There are four parameters in the proposed model (modified Exponential and modified Gaussian) that are varied in the exhaustive search for a best-fit. The values of σ/T and σ'/T' are made equal in this search. The ranges for the parameters used in the experiment are: $\sigma/T = \sigma'/T'$ which ranges from [0.12, 4.1] with 50 equal intervals, β which ranges from [0.01, 1] with 100 equal intervals, the index of refraction, with a range of [1.3, 1.5] with 10 equal intervals, and a with a range of [0, 1] with 101 equal intervals. The range for ϕ_a and ϕ_s for the Jensen model [10] are varied between [0.01, 1] with 100 intervals. Meanwhile, for the Oren-Nayar model [12], the parameter values were chosen based on the tabulated data given, but using only the diffuse component. The results are shown as plots of normalized measured data versus the normalized radiance predicted by the different models. The fitting and parameter estimation results are shown in Table II-IV.

B. Chi-Square per Degree of Freedom Test

To measure the discrepancy existing between the best-fit error (observation data) and its expected error, the chi-square per degree of freedom test was used to check whether the Ragheb-Hancock model and the absorption model differ significantly. The Chi-squared statistic is given by:

$$\chi^2 = \sum_{n=1}^{198} \frac{(Model_n - Data_n)^2}{Data_n} \quad (16)$$

After obtaining the chi-squared statistic, it is then divided by v the number of degrees of freedom to give χ^2/v the chi-squared per degree of freedom, where $v = d - p$. Here, $d = 198$ which is the number of data samples and p is the number of model parameters. For the Ragheb-Hancock model, $p = 3$ while the proposed model has $p = 4$. A comparison of the Ragheb-Hancock model and the proposed absorption model is given in Table V.

V. DISCUSSION

From the best-fit models and their associated parameters, there are several conclusions that can be drawn

- 1) When the absorption fraction a in the modified absorption model is zero, the model is equivalent the Ragheb-Hancock model.
- 2) The modified absorption model gave the best-fit overall. The Jensen model overestimated the radiance data while the Oren-Nayar model underestimated it.
- 3) A total of 7 samples gave the best fit when the absorption was zero. However, a total of 6 chromatic samples gave better results using the proposed absorption model; these samples were Rug-B (red), velvet (red), Quarry tile (pale red), Brown bread, Orange peel and Moss (green). This shows that the proposed model accounts well for chromatics effects in colored samples.
- 4) For samples that are dominated by one colour, e.g. Rug-B - red, the parameters σ/T and β are larger and the parameter a is smaller in the dominant color channel.
- 5) The velvet sample gives the poorest fit of all the samples for both the modified Exponent and Gaussian models. This is probably due to measurement noise. Nevertheless, the proposed model still gave the best fit compared to the alternative models.
- 6) The absorption model variant with an exponential correlation function gives the best overall fit for all 13 samples on all color channels, followed by the absorption model variant with a Gaussian correlation function.
- 7) There is no significant difference between the chi-square test for the Ragheb-Hancock model and the proposed absorption model.

In comparison to the Ragheb-Hancock model, the new absorption model provides improvements in the quality of fit while allowing us to estimate the absorption fraction a , thus providing information concerning the absorption characteristics of the incident light.

TABLE II
THE RMS FIT ERROR Δ_{RMS} CORRESPONDING TO THE MODELS STUDIED FOR 13 CURET SAMPLES.

Sample (no.)	Exp_R	$Gaus_R$	Jen_R	ON_R	Exp_G	$Gaus_G$	Jen_G	ON_G	Exp_B	$Gaus_B$	Jen_B	ON_B
Felt (1)	0.4614	0.5205	2.6657	3.0177	0.4282	0.4818	2.8145	2.5626	0.5413	0.5945	1.8640	3.7595
Terry Cloth (3)	0.5159	0.5440	1.5696	3.7849	0.5064	0.5319	1.5582	3.7940	0.5052	0.5250	1.5383	3.8126
Velvet (7)	1.3626	1.0220	3.2774	1.5568	0.8966	0.9469	5.0024	0.6819	0.9171	0.9501	4.9259	6.1236
Rug-A (18)	0.4203	0.4812	2.3808	2.7587	0.4006	0.4659	2.4446	2.8536	0.3693	0.4347	2.8100	2.4729
Rug-B (19)	0.6179	0.4420	3.1501	1.4729	0.3251	0.3188	4.5258	1.0338	0.3315	0.3312	4.5200	1.0381
Sponge (21)	0.3180	0.3819	2.0959	2.4739	0.2569	0.3127	2.8727	2.4632	0.2112	0.2662	3.7463	1.6272
Quarry Tile (25)	0.4368	0.4808	3.6416	1.2946	0.3786	0.3935	4.5629	1.1512	0.3716	0.3853	4.7954	6.3168
Brown Bread (48)	0.3736	0.4523	2.6015	2.3133	0.3585	0.4373	3.0615	2.3286	0.3047	0.3747	3.7275	1.7031
Corn Husk (51)	0.6466	0.6626	1.8945	3.1789	0.6546	0.6767	1.9531	3.5755	0.4938	0.5131	3.1144	2.2818
White Bread (52)	0.4276	0.5038	1.5637	3.8676	0.4166	0.5050	1.6230	3.8585	0.3774	0.4737	2.0420	3.3901
Soleirolia Plant (53)	0.4507	0.5015	3.3256	2.1832	0.5563	0.5985	2.6582	2.7362	0.3809	0.4348	3.7405	1.6787
Orange Peel (55)	0.7394	0.7915	2.8696	1.2485	0.3794	0.4500	4.6247	0.9470	0.3204	0.3662	5.2467	0.4896
Moss (61)	0.4102	0.3386	4.3900	1.2580	0.3767	0.3265	4.2371	1.3651	0.6432	0.5678	4.4290	1.3021

TABLE III
THE MODEL PARAMETERS ESTIMATED FOR THE MODIFIED *Exponential* MODEL, CORRESPONDING TO THE RMS FIT ERRORS FOR THE 13 CURET SAMPLES.

Sample (No.)	Red Channel				Green Channel				Blue Channel			
	σ/T	β	n	a	σ/T	β	n	a	σ/T	β	n	a
Felt (1)	1.24	0.34	1.50	0.00	1.40	0.31	1.50	0.00	1.56	0.44	1.50	0.00
Terry Cloth (3)	4.04	0.63	1.50	0.00	4.04	0.63	1.50	0.00	4.04	0.63	1.50	0.00
Velvet (7)	4.04	0.28	1.50	0.00	3.24	0.01	1.50	1.00	4.04	0.01	1.50	1.00
Rug-A (18)	2.12	0.36	1.50	0.00	2.20	0.35	1.50	0.00	2.20	0.30	1.50	0.00
Rug-B (19)	4.04	0.31	1.30	0.48	4.04	0.01	1.30	1.00	4.04	0.01	1.30	1.00
Sponge (21)	3.80	0.40	1.50	0.00	3.80	0.31	1.50	0.00	3.56	0.17	1.44	0.00
Quarry Tile (25)	0.84	0.24	1.50	0.29	0.68	0.12	1.30	0.82	0.68	0.01	1.30	1.00
Brown Bread (48)	2.20	0.34	1.30	0.03	1.96	0.28	1.30	0.18	1.72	0.18	1.30	0.35
Corn Husk (51)	1.32	0.55	1.50	0.00	1.24	0.54	1.50	0.00	1.4	0.26	1.50	0.00
White Bread (52)	2.12	0.50	1.50	0.00	2.04	0.47	1.50	0.00	2.28	0.40	1.50	0.00
Soleirolia Plant (53)	2.36	0.24	1.50	0.00	3.80	0.34	1.50	0.00	1.64	0.16	1.50	0.00
Orange Peel (55)	0.84	0.36	1.50	0.00	0.44	0.10	1.50	0.26	0.28	0.01	1.30	1.00
Moss (61)	4.04	0.07	1.30	1.00	4.04	0.11	1.30	1.00	4.04	0.05	1.30	1.00

TABLE IV
THE MODEL PARAMETERS ESTIMATED FOR THE MODIFIED *Gaussian* MODEL, CORRESPONDING TO THE RMS FIT ERRORS FOR THE 13 CURET SAMPLES.

Sample (No.)	Red Channel				Green Channel				Blue Channel			
	σ/T	β	n	a	σ/T	β	n	a	σ/T	β	n	a
Felt (1)	0.60	0.34	1.50	0.00	0.68	0.30	1.50	0.00	0.68	0.44	1.50	0.00
Terry Cloth (3)	2.36	0.65	1.50	0.00	2.36	0.65	1.50	0.00	2.36	0.65	1.50	0.00
Velvet (7)	4.04	0.28	1.50	0.00	1.96	0.01	1.50	1.00	2.36	0.01	1.50	1.00
Rug-A (18)	0.92	0.34	1.50	0.00	0.92	0.33	1.50	0.00	0.92	0.28	1.50	0.00
Rug-B (19)	3.64	0.27	1.42	0.36	2.36	0.01	1.50	1.00	2.28	0.01	1.50	1.00
Sponge (21)	1.96	0.39	1.50	0.00	1.88	0.29	1.50	0.00	1.64	0.13	1.50	0.00
Quarry Tile (25)	0.44	0.23	1.50	0.37	0.36	0.10	1.30	0.86	0.36	0.01	1.50	1.00
Brown Bread (48)	1.08	0.31	1.30	0.00	1.08	0.25	1.30	0.07	0.84	0.16	1.30	0.39
Corn Husk (51)	0.60	0.55	1.50	0.00	0.60	0.53	1.50	0.00	0.68	0.25	1.50	0.00
White Bread (52)	0.84	0.51	1.50	0.00	0.84	0.48	1.48	0.00	1.00	0.38	1.50	0.00
Soleirolia Plant (53)	1.08	0.20	1.50	0.00	1.96	0.33	1.50	0.00	0.84	0.14	1.50	0.00
Orange Peel (55)	0.44	0.35	1.50	0.00	0.28	0.08	1.50	0.41	0.20	0.01	1.30	1.00
Moss (61)	2.92	0.05	1.30	1.00	2.84	0.09	1.30	0.87	3.08	0.03	1.30	1.00

VI. CONCLUSION

In this paper, we have introduced a new light scattering model for layered rough surfaces with absorption. For the CURET database, we demonstrate that the method offers improvements over a number of alternative light scattering models including the Ragheb-Hancock model, which is an absorption-free version of the new method. The new method handles wavelength dependant chromatic absorption effects, which are beyond the scope of the Ragheb-Hancock model. The new model extends the Ragheb-Hancock model not only

for the purposes of analyzing subsurface roughness, but also for analyzing the absorption characteristics of surfaces. This is a significant advantage when studying biological materials such as the skin and plant leaf. In the future, further experiments will be conducted on both highly chromatic and biological materials.

REFERENCES

- [1] H. Ragheb and E. R. Hancock, "A light scattering model for layered dielectrics with rough surface boundaries," *International Journal of*

TABLE V
THE CHI-SQUARE TEST PER DEGREE OF FREEDOM FOR THE 13 CURET SAMPLES.

Sample (No.)	Modified Model						Ragheb Model					
	Exponent			Gaussian			Exponent			Gaussian		
	R	G	B	R	G	B	R	G	B	R	G	B
Felt (1)	0.0327	0.0369	0.0378	0.0419	0.0493	0.0482	0.0327	0.0367	0.0376	0.0417	0.0491	0.0480
Terry Cloth (3)	0.0115	0.0112	0.0111	0.0128	0.0123	0.0118	0.0114	0.0112	0.0111	0.0127	0.0123	0.0118
Velvet (7)	0.0633	0.1328	0.2049	0.0442	0.1500	0.2161	0.0630	0.1332	0.2077	0.0440	0.1496	0.2183
Rug-A (18)	0.0293	0.0242	0.0193	0.0596	0.0546	0.0445	0.0291	0.0241	0.0192	0.0593	0.0543	0.0443
Rug-B (19)	0.0193	0.0131	0.0135	0.0101	0.0126	0.0133	0.0314	0.0140	0.0143	0.0146	0.0131	0.0136
Sponge (21)	0.0052	0.0040	0.0039	0.0160	0.0111	0.0187	0.0052	0.0040	0.0039	0.0159	0.0111	0.0186
Quarry Tile (25)	0.0238	0.0116	0.0206	0.0275	0.0149	0.0199	0.0256	0.0228	0.0229	0.0320	0.0268	0.0226
Brown Bread (48)	0.0205	0.0189	0.0120	0.0512	0.0438	0.0220	0.0208	0.0227	0.0162	0.0520	0.0454	0.0278
Corn Husk (51)	0.0298	0.0294	0.0240	0.0272	0.0288	0.0219	0.0297	0.0293	0.0239	0.0271	0.0286	0.0218
White Bread (52)	0.0438	0.0381	0.0731	0.0746	0.0623	0.1845	0.0436	0.0379	0.0728	0.0743	0.0620	0.1836
Soleirolia Plant (53)	0.0231	0.0183	0.0182	0.0588	0.0247	0.0285	0.0230	0.0182	0.0181	0.0585	0.0246	0.0283
Orange Peel (55)	0.0912	0.0218	0.0255	0.0962	0.0296	0.0424	0.0907	0.0220	0.0277	0.0957	0.0305	0.0457
Moss (61)	0.0122	0.0112	0.0356	0.0083	0.0083	0.0287	0.0231	0.0261	0.0461	0.0116	0.0136	0.0321

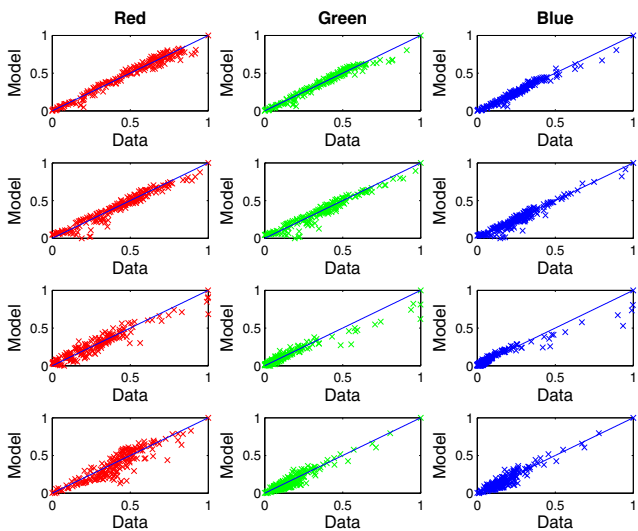


Fig. 3. CURET samples: normalized data against the normalized radiance predicted by the modified Exponential model. Samples from top to bottom are: Sponge (21), Brown Bread (48), Quarry Tile (25), Rug-B (19).

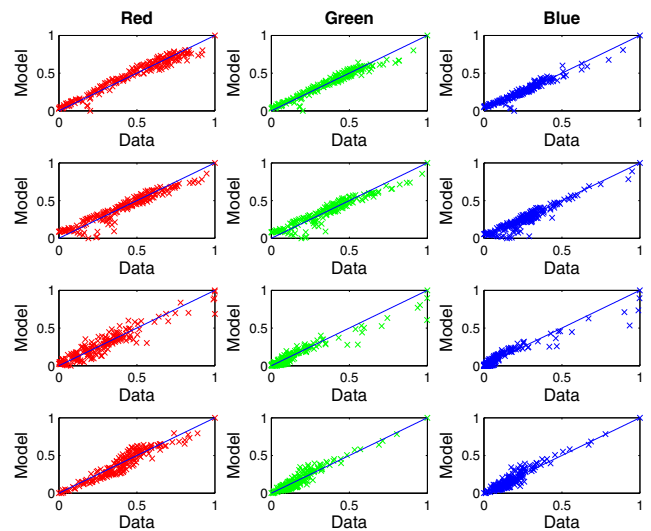


Fig. 4. CURET samples: normalized data against the normalized radiance predicted by the modified Gaussian model. Samples from top to bottom are: Sponge (21), Brown Bread (48), Quarry Tile (25), Rug-B (19).

Computer Vision, vol. 79, no. 2, pp. 179–207, 2007. [Online]. Available: <http://dx.doi.org/10.1007/s11263-007-0113-5>

[2] M. Kurt and D. Edwards, “A survey of brdf models for computer graphics,” *SIGGRAPH Comput. Graph.*, vol. 43, no. 2, pp. 4:1–4:7, May 2009. [Online]. Available: <http://doi.acm.org/10.1145/1629216.1629222>

[3] R. Montes and C. Ureña, “An overview of brdf models,” *University of Grenada, Technical Report LSI-2012-001*, 2012.

[4] K. E. Torrance and E. M. Sparrow, “Theory for off-specular reflection from roughened surfaces,” *J. Opt. Soc. Am.*, vol. 57, no. 9, pp. 1105–1114, Sep 1967. [Online]. Available: <http://www.osapublishing.org/abstract.cfm?URI=josa-57-9-1105>

[5] M. Oren and S. K. Nayar, “Generalization of the lambertian model and implications for machine vision,” *Int. J. Comput. Vision*, vol. 14, no. 3, pp. 227–251, Apr. 1995. [Online]. Available: <http://dx.doi.org/10.1007/BF01679684>

[6] J. Stam, *Rendering Techniques 2001: Proceedings of the Eurographics Workshop in London, United Kingdom, June 25–27, 2001*. Vienna: Springer Vienna, 2001, ch. An Illumination Model for a Skin Layer Bounded by Rough Surfaces, pp. 39–52. [Online]. Available: http://dx.doi.org/10.1007/978-3-7091-6242-2_4

[7] W. Matusik, H. Pfister, M. Brand, and L. McMillan, “A data-driven reflectance model,” *ACM Trans. Graph.*, vol. 22, no. 3, pp. 759–769, Jul. 2003. [Online]. Available: <http://doi.acm.org/10.1145/882262.882343>

[8] T. Igarashi, K. Nishino, and S. K. Nayar, “The appearance of human skin: A survey,” *Foundations and Trends® in Computer Graphics and Vision*, vol. 3, no. 1, pp. 1–95, 2007.

[9] C. Donner, T. Weyrich, E. d’Eon, R. Ramamoorthi, and S. Rusinkiewicz, “A layered, heterogeneous reflectance model for acquiring and rendering human skin,” *ACM Trans. Graph.*, vol. 27, no. 5, pp. 140:1–140:12, Dec. 2008. [Online]. Available: <http://doi.acm.org/10.1145/1409060.1409093>

[10] H. W. Jensen, S. R. Marschner, M. Levoy, and P. Hanrahan, “A practical model for subsurface light transport,” in *Proceedings of the 28th Annual Conference on Computer Graphics and Interactive Techniques*, ser. SIGGRAPH ’01. New York, NY, USA: ACM, 2001, pp. 511–518. [Online]. Available: <http://doi.acm.org/10.1145/383259.383319>

[11] C. F. Bohren and D. R. Huffman, *Absorption and scattering of light by small particles*. John Wiley & Sons, 2008.

[12] K. J. Dana, B. van Ginneken, S. K. Nayar, and J. J. Koenderink, “Reflectance and texture of real-world surfaces,” *ACM Trans. Graph.*, vol. 18, no. 1, pp. 1–34, Jan. 1999. [Online]. Available: <http://doi.acm.org/10.1145/300776.300778>